Articles

Methanol Bonding to and Electron-Transfer Reactivity of Chloro(tetraphenylporphinato)manganese(III)

Xi Hai Mu and Franklin A. Schultz*

Department of Chemistry, Indiana University-Purdue University at Indianapolis, 1125 East 38th Street, Indianapolis, Indiana 46205-2810

Received December 17, 1991

The ability of axial ligation to modulate redox potentials and electrode half-reactions of metalloporphyrins is illustrated by coordination of methanol to Mn(TPP)Cl (**1**) and its reduced and oxidized products in 1,2-dichloroethane. Visible spectrophotometry, spectroelectrochemistry, and cyclic and microelectrode voltammetry are used to characterize reactions whereby six-coordinate Mn(III) [Mn(TPP)(CH_3OH)Cl (**3**) and Mn(TPP)(CH_3OH)$_2^+$ (**4**)] and five-coordinate Mn(II) [Mn(TPP)(CH_3OH) (**6**)] species are formed from **1**. The axial ligand preferences of these two oxidation states lead to a biphasic behavior in the potential of $Mn^{III/II}$ reduction. At low CH_3OH concentrations, five-coordinate **1** is reduced to five-coordinate **6**, causing $E_{1/2}$ to shift to positive values with increasing [CH_3OH]; at larger methanol concentrations, reduction of **4** to **6** predominates and the shift is in the opposite direction. In addition, the ring- and metal-centered oxidations of **1** at 1.22 and 1.56 V vs Ag/AgCl, respectively, coalesce into a single two-electron process at 1.31 V upon CH_3OH coordination. The negative shift in the metal-centered oxidation potential is an anticipated consequence of the greater donor strength of two CH_3OH ligands versus one Cl^- ligand. The positive shift in the ring-centered potential is believed to result from reduced deformation of the porphyrin core and consequent stabilization of the porphyrin HOMO as axial coordination by CH_3OH returns the Mn atom to an in-plane position from its significant out-of-plane displacement (0.27 Å) in **1**.

Introduction

Manganese porphyrins[1] are of interest as homogeneous catalysts of hydrocarbon oxygenation,[2-6] as models for similar reactivity in the heme protein cytochrome P-450,[7,8] as reagents for intercalation and cleavage of DNA,[9] and as active components in membrane electrodes that display unusual anion selectivities.[10] Five-coordinate chloro(tetraphenylporphinato)manganese(III), Mn(TPP)Cl (**1**), which exhibits a 0.27-Å Mn atom out-of-plane displacement,[11a] has been studied extensively in this regard. Key to the role of Mn(TPP)Cl in many of its reactions and a point of general interest in metalloporphyrin chemistry is the extent to which redox and catalytic properties are altered by changes in axial ligation. A long-standing question[12-15] concerns the result of adding neutral Lewis base ligands to structures such as **1** and whether the favored products are five-coordinate, ligand-substituted (**2**), six-coordinate, mixed-ligand (**3**), or six-coordinate,

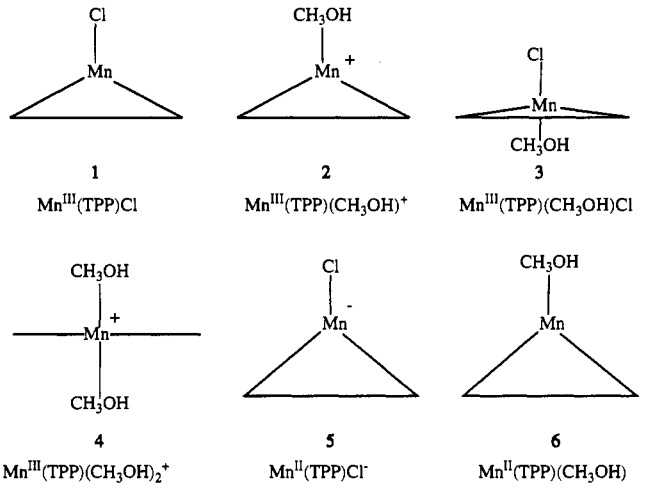

(1) (a) Boucher, L. J. *Coord. Chem. Rev.* **1972**, *7*, 289. (b) Boucher, L. J. *Ann. N.Y. Acad. Sci.* **1973**, *206*, 409. (c) Scheidt, W. R. *Acc. Chem. Res.* **1977**, *10*, 339.
(2) (a) Powell, M. F.; Pai, E. F.; Bruice, T. C. *J. Am. Chem. Soc.* **1984**, *106*, 3277. (b) Yuan, L.-C.; Bruice, T. C. *J. Am. Chem. Soc.* **1986**, *108*, 1643.
(3) (a) Collman, J. P.; Brauman, J. I.; Meunier, B.; Hayashi, T.; Raybuck, S. A. *J. Am. Chem. Soc.* **1985**, *107*, 2000. (b) Collman, J. P.; Kodadek, T.; Raybuck, S. A.; Meunier, B. *Proc. Natl. Acad. Sci. U.S.A.* **1983**, *80*, 7039.
(4) (a) Groves, J. T.; Kruper, W. J., Jr.; Haushalter, R. C. *J. Am. Chem. Soc.* **1980**, *102*, 6375. (b) Groves, J. T.; Watanabe, Y.; McMurry, T. J. *J. Am. Chem. Soc.* **1983**, *105*, 4489. (c) Groves, J. T.; Stern, M. K. *J. Am. Chem. Soc.* **1988**, *110*, 8628.
(5) (a) Hill, C. L.; Schardt, B. C. *J. Am. Chem. Soc.* **1980**, *102*, 6374. (b) Smegal, J. A.; Schardt, B. C.; Hill, C. L. *J. Am. Chem. Soc.* **1983**, *105*, 3510. (c) Williamson, M. W.; Hill, C. L. *Inorg. Chem.* **1986**, *25*, 4668. (d) Brown, R. B., Jr.; Williamson, M. W.; Hill, C. L. *Inorg. Chem.* **1987**, *26*, 1602.
(6) (a) Creager, S. E.; Raybuck, S. A.; Murray, R. W. *J. Am. Chem. Soc.* **1986**, *108*, 4225. (b) Creager, S. E.; Murray, R. W. *Inorg. Chem.* **1987**, *26*, 2612.
(7) *Cytochrome P-450: Structure, Mechanism and Biochemistry*; Ortiz de Montellano, P., Ed.; Plenum Press: New York, 1986.
(8) Mansuy, D.; Battioni, T.; Battioni, J. P. *Eur. J. Biochem.* **1989**, *184*, 267.
(9) (a) Pasternak, R. F.; Gibbs, E. J.; Villafranca, J. S. *Biochemistry* **1983**, *22*, 2406. (b) Ward, B.; Skorobogaty, A.; Dabrowiak, J. C. *Biochemistry* **1986**, *25*, 6875. (c) Rodriguez, M.; Kodadek, T.; Torres, M.; Bard, A. J. *Bioconjugate Chem.* **1990**, *1*, 123.
(10) (a) Ammann, D.; Huser, M.; Kraulter, B.; Rusterholz, B.; Schulthess, P.; Lindemann, B.; Halder, E.; Simon, W. *Helv. Chim. Acta* **1986**, *69*, 849. (b) Chaniotakis, N. A.; Chasser, A. M.; Meyerhoff, M. E. *Anal. Chem.* **1988**, *60*, 185.
(11) (a) Tulinsky, A.; Chen, B. M. L. *J. Am. Chem. Soc.* **1977**, *99*, 3647. (b) Van Atta, R. B.; Strouse, C. E.; Hanson, L. K.; Valentine, J. S. *J. Am. Chem. Soc.* **1987**, *109*, 1425.
(12) (a) LaMar, G. N.; Walker, F. A. *J. Am. Chem. Soc.* **1975**, *97*, 5103. (b) Walker, F. A.; Lo, M.-W.; Ree, T. F. *J. Am. Chem. Soc.* **1976**, *98*, 5552.
(13) (a) Kadish, K. M.; Kelly, S. *Inorg. Chem.* **1979**, *18*, 2968. (b) Kelly, S. L.; Kadish, K. M. *Inorg. Chem.* **1982**, *21*, 3631.
(14) (a) Neya, S.; Morishima, I.; Yonezawa, T. *Biochemistry* **1981**, *20*, 2610. (b) Goff, H. M.; Hansen, A. P. *Inorg. Chem.* **1984**, *23*, 321.

0020-1669/92/1331-3351$03.00/0

bisligated (4) species. Structure 3 is of particular interest because it is reported to be an intermediate in catalytic oxygenations by Mn(TPP)Cl[2,3a,4a] (bisligated forms have little or no effect) and the species responsible for the anion selectivity of Mn–porphyrin membrane electrodes.[10b] X-ray crystal structures of isolated complexes of this form have been reported [e.g., Mn(TPP)(CH_3OH)N_3[16] and Mn(TPP)(Py)Cl[17]], but their existence in solution has been difficult to document.

This paper presents the results of electrochemical and spectroscopic studies of CH_3OH bonding to Mn(TPP)Cl in the noncoordinating solvent 1,2-dichloroethane. Methanol was selected as representative of the oxygen-donor ligands that are important in the oxidative and catalytic chemistry of manganese porphyrins.[18-20] Formation of structures 3 and 4 results in significant changes in electrochemical and spectroscopic properties relative to 1. Thus, methanol coordination is an effective vehicle for understanding relationships between axial ligation and the physical properties of metalloporphyrins that may be important in their catalytic and biological reactivity.

Experimental Section

Reagents. Mn(TPP)Cl was purchased from Aldrich Chemical Co. and used as received. It exhibited the following spectral features [λ_{max}, nm (ϵ, M^{-1} cm^{-1})]: in 1,2-dichloroethane, 476 (113 000), 532 (6090), 582 (9980), 620 (11 700); in methanol, 466 (89 500), 518 (7080), 566 (11 600), 600 (8700). The absorption spectrum of Mn(TPP)Cl in methanol is in good agreement with that of the isolated complex [Mn(TPP)(CH_3OH)$_2$]ClO_4·CH_3OH.[21] 1,2-Dichloroethane (Aldrich) was distilled from P_2O_5. Spectrophotometric grade methanol (Aldrich) was used as received. Tetra-*n*-butylammonium tetrafluoroborate (Bu_4NBF_4) from Southwestern Analytical Chemicals was used as supporting electrolyte in electrochemical experiments. Tetraethylammonium chloride (Et_4NCl) from Kodak was dried by dissolving the salt in CH_2Cl_2 and passing the solution through a column filled with Na_2SO_4. CH_2Cl_2 was evaporated from the eluate by a stream of argon, and the salt was stored at 80 °C under vaccum.

Equipment and Procedures. Electrochemical measurements were carried out with an IBM EC-225 voltammetric analyzer. The cell design for voltammetric measurements has been reported.[22] Conventional cyclic voltammetry was carried out at a 1.6 mm diameter Pt disk working electrode with the tip of the reference electrode salt bridge positioned at a distance of 0.5 mm and positive feedback employed to reduce *iR* drop loss. Steady-state voltammograms were recorded at a 25 μm diameter Pt disk microelectrode. The auxiliary electrode was a coaxial Pt coil, and the reference electrode was an aqueous Ag/AgCl (3 M KCl) half-cell immersed in a salt bridge containing supporting electrolyte. Ferrocene oxidation was observed at a potential of 0.49 V versus this reference electrode in 0.1 M Bu_4NBF_4/$ClCH_2CH_2Cl$. Voltammetric measurements were carried out at temperatures controlled to ±0.2 °C with an FTS Multi-Cool system. Spectroscopic and spectroelectrochemical measurements were carried out at an ambient temperature of 23 ± 0.5 °C.

The design of the thin-layer spectroelectrochemical cell is described in ref 23. The working electrode was constructed from 52-gauge platinum mesh (Fisher Scientific), and the reference electrode was an aqueous Ag/AgCl (3 M KCl) half-cell. The optical path length of the cell was 0.2 mm. Spectrophotometric measurements were made with a Hewlett Packard 8450A diode array spectrophotometer with 0.1 and 1.0 cm path length cells. Conductance measurements were made with a YSI Model 31 conductance bridge and a homemade cell containing 0.8-cm^2 Pt flags positioned 0.35 cm from one another. The cell constant (l/A) determined in aqueous 0.01 M KCl was 0.414 cm^{-1}.

Spectrophotometric and conductometric titrations were carried out by mixing $ClCH_2CH_2Cl$ and methanol solutions containing equal concentrations of Mn(TPP)Cl to avoid dilution effects. The same procedure was followed for the voltammetrically monitored titrations, except that both solutions also contained 0.1 M Bu_4NBF_4 or 0.1 M Et_4NCl.

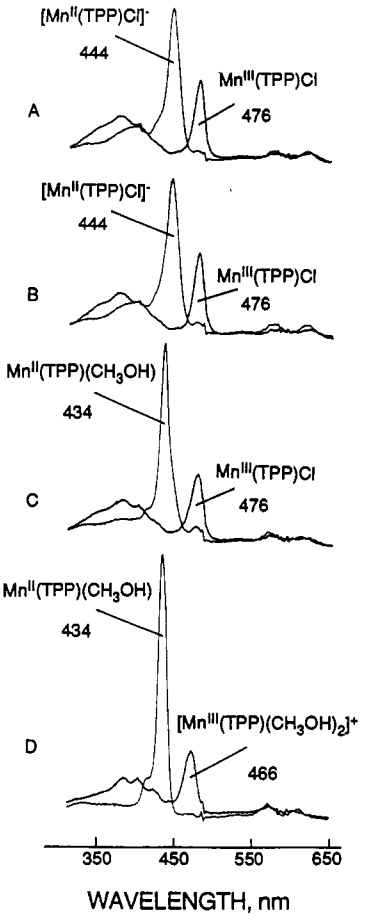

Figure 1. Thin-layer spectra recorded before and after controlled-potential reduction at –0.4 V of 5.7 × 10^{-5} M Mn(TPP)Cl in $ClCH_2CH_2Cl$ containing 0.1 M Bu_4NBF_4 and (A) 0.0, (B) 0.092, (C) 0.395, and (D) 3.06 M methanol.

Results

Electrochemical and Spectroscopic Studies of CH_3OH Bonding to Mn(TPP)Cl. A clear description of CH_3OH bonding to Mn(TPP)Cl is provided by spectroelectrochemical experiments carried out in the Soret band region before and after one-electron reduction of the metal center in the presence of varying amounts of methanol. The results are shown in Figure 1. In addition, the half-wave potential of $Mn^{III/II}$ reduction determined as the average of cathodic and anodic peak potentials by cyclic voltammetry in 0.1 M Et_4NCl is plotted as a function of methanol concentration in Figure 2. At [CH_3OH] < 0.1 M (Figure 1A,B), the spectrum of Mn(TPP)Cl remains unchanged and the spectrum of the Mn^{II} electrode product exhibits a Soret band maximum at 444 nm. The latter feature is found in the spectra of five-coordinate Mn(II) porphyrins that are axially coordinated by an anionic ligand, and its energy is distinctly less than that of the absorptions of Mn(II) porphyrins that are four-coordinate or are axially ligated by solvent or a neutral ligand ($\lambda_{max} \cong$ 437 nm).[24] In addition,

(15) (a) Adams, K. M.; Rasmussen, P. G.; Scheidt, W. R.; Hatano, K. *Inorg. Chem.* **1979**, *18*, 1892. (b) Byers, W.; Cossham, J. A.; Edwards, J. O.; Gordon, A. T.; Jones, J. G.; Kenny, E. T. P.; Mahmood, A.; McKnight, J.; Sweigart, D. A.; Tondreau, G. A.; Wright, T. *Inorg. Chem.* **1986**, *25*, 4767.
(16) (a) Day, V. W.; Stults, B. R.; Tasset, E. L.; Day, R. O.; Marianelli, R. S. *J. Am. Chem. Soc.* **1974**, *96*, 2650. (b) Day, V. W.; Stults, B. R.; Tasset, E. L.; Marianelli, R. S.; Boucher, L. J. *Inorg. Nucl. Chem. Lett.* **1975**, *11*, 505.
(17) Kirner, J. F.; Scheidt, W. R. *Inorg. Chem.* **1975**, *14*, 2081.
(18) (a) Hill, C. L.; Williamson, M. W. *Inorg. Chem.* **1985**, *24*, 2836. (b) *Inorg. Chem.* **1985**, *24*, 3024.
(19) Balasubramanian, P. N.; Schmidt, E. S.; Bruice, T. C. *J. Am. Chem. Soc.* **1987**, *109*, 7865.
(20) Robert, A.; Loock, B.; Momenteau, M.; Meunier, B. *Inorg. Chem.* **1991**, *30*, 706.
(21) Hatano, K.; Anzai, K.; Iitaka, Y. *Bull. Chem. Soc. Jpn.* **1983**, *56*, 422.
(22) Mu, X. H.; Schultz, F. A. *Electroanalysis* **1990**, *2*, 353.
(23) Lin, X. Q.; Kadish, K. M. *Anal. Chem.* **1985**, *57*, 1498.
(24) Arasasingham, R. D.; Bruice, T. C. *Inorg. Chem.* **1990**, *29*, 1422.

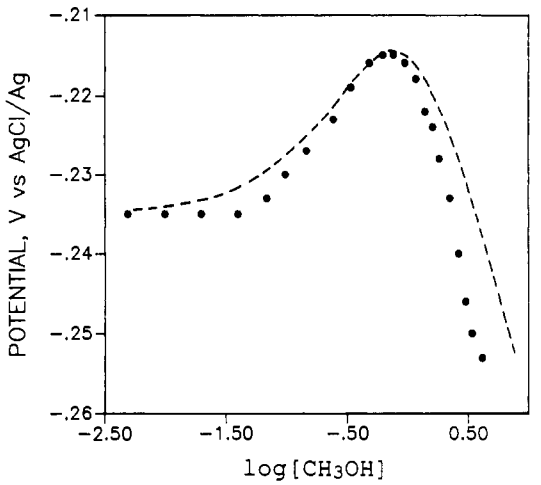

Figure 2. Dependence of the half-wave potential of $Mn^{III}(TPP)Cl$ reduction on methanol concentration in $ClCH_2CH_2Cl$ containing 0.1 M Et_4NCl (T = 296 K): (●) experimental data; (- -) data calculated using eq 10 and $(E_{1/2})_0$ = –0.235 V, K_1^{II} = 0.4, K_1^{III} = 0.3 M^{-1}, β_2^{III} = 1.0 M^{-2}, and $[Cl^-]$ = 0.1 M.

the half-wave potential of Mn(III) reduction remains independent of added methanol. From these results we conclude that the one-electron reduction of Mn(TPP)Cl at $[CH_3OH] < 0.1$ M proceeds to the five-coordinate product, **5** (eq 1). This conclusion

$$Mn^{III}(TPP)Cl + e^- \rightleftharpoons Mn^{II}(TPP)Cl^- \quad (1)$$

is supported by the fact that $Mn(TPP)Cl^-$ has been isolated as a solid and its X-ray crystal structure determined.[11b] The axial chloride ligand is retained, and the displacement of the Mn atom above the porphyrin plane increases from 0.27 to 0.64 Å upon reduction.

At CH_3OH concentrations between approximately 0.1 and 1.0 M, some changes occur in the spectrum of Mn(TPP)Cl. The Soret band maximum remains at 476 nm, but decreases in absorbance occur at this wavelength (Figure 3A) and at the wavelengths of the lower energy absorption bands (data not shown). The absorption maximum of the reduced product changes to 434 nm (Figure 1C), which is characteristic of a five-coordinate Mn(II) porphyrin with a neutral axial ligand.[24] Over this range of CH_3OH concentrations, the half-wave potential of Mn(III) reduction shifts in the positive direction with a slope of ca. 25 mV versus log $[CH_3OH]$ (Figure 2) and the molar conductance of the solutions is negligible. These results are consistent with an electrode reaction in which the chloride ion remains bound to the oxidized reactant and one molecule of methanol is added to the reduced product. Given the strong preference of Mn(II) porphyrins for five-coordination,[1c,25] reduction of Mn(TPP)Cl under these conditions is assumed to proceed via reactions 2 and 3 to a product in which the axial chloride ligand is replaced by CH_3OH (**6**).

$$Mn^{III}(TPP)Cl + CH_3OH + e^- \rightleftharpoons Mn^{II}(TPP)(CH_3OH) + Cl^- \quad (2)$$

$$Mn^{III}(TPP)(CH_3OH)Cl + e^- \rightleftharpoons Mn^{II}(TPP)(CH_3OH) + Cl^- \quad (3)$$

At CH_3OH concentrations above 1.0 M, the absorption spectrum of Mn(TPP)Cl changes dramatically. These changes are effectively complete at $[CH_3OH] \simeq 3$ M and result in a shift of the Soret band maximum to 466 nm (Figures 1D and 3B).

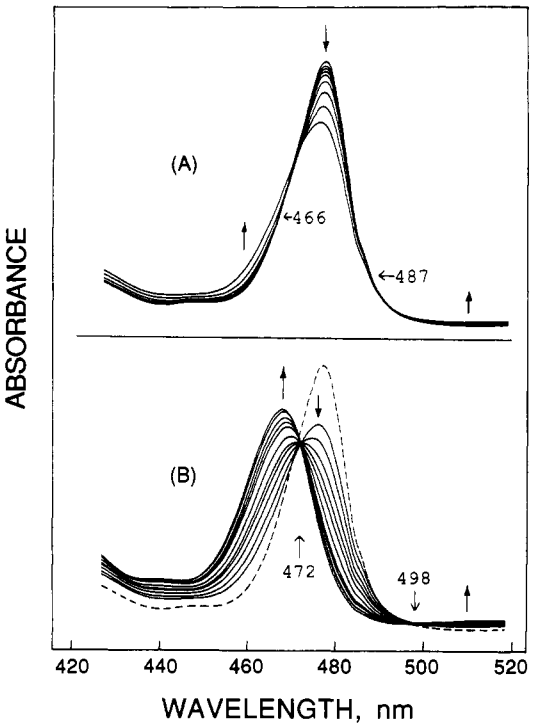

Figure 3. Spectral changes observed during titration of 7.6×10^{-6} M Mn(TPP)Cl with CH_3OH in $ClCH_2CH_2Cl$: (A) $[CH_3OH]$ = 0.0–0.40 M (466- and 487-nm isosbestic points marked by arrows); (B) $[CH_3OH]$ = 0.40–10.5 M (472- and 498-nm isosbestic points marked by arrows and spectrum of Mn(TPP)Cl in absence of methanol shown as dashed line).

This spectral feature is identical with the Soret band of $Mn(TPP)(CH_3OH)_2^+$.[21] The spectrum of the Mn(II) electrode product remains unchanged from that at intermediate methanol concentrations and retains its Soret band maximum at 434 nm (Figure 1D). At these larger CH_3OH concentrations, $E_{1/2}$ shifts in the negative direction with increasing $[CH_3OH]$, and the slope of the $E_{1/2}$ vs log $[CH_3OH]$ plot is –59 mV (Figure 2). Under these experimental conditions, $Mn(TPP)Cl/ClCH_2CH_2Cl$ solutions exhibit some conductivity. However, the molar conductance at 3 M CH_3OH corresponds to only ~30% of the value observed for a 1:1 electrolyte in a solvent of this composition. Thus, we conclude that $Mn(TPP)(CH_3OH)_2^+Cl^-$ remains almost fully ion-paired during the spectroscopic titration[26] and that the electrode reaction at 1–3 M CH_3OH involves reduction of six-coordinate Mn(III) (**4**) to five-coordinate Mn(II) (**6**) accompanied by release of one molecule of methanol.

$$Mn^{III}(TPP)(CH_3OH)_2^+Cl^- + e^- \rightleftharpoons Mn^{II}(TPP)(CH_3OH) + CH_3OH + Cl^- \quad (4)$$

Stability constants for binding of CH_3OH to Mn(TPP)Cl were determined from Benesi–Hildebrand plots:[27]

$$\log [(A_0 - A)/(A - A_\infty)] = n \log [CH_3OH] + \log \beta_n \quad (5)$$

where A_0 is the absorbance of Mn(TPP)Cl, A_∞ is the absorbance of the fully formed complex with methanol, and A is the absorbance of the equilibrium mixture. The slopes, n, of such plots indicate the number of molecules of CH_3OH coordinated, and the intercepts provide the equilibrium constants K_1^{III} and β_2^{III} corresponding to reactions 6 and 7, respectively. Results obtained at porphyrin concentrations between 7.6×10^{-6} and 8.5×10^{-4}

(25) (a) Gonzalez, B.; Kouba, J.; Yee, S.; Reed, C. A.; Kirner, J. F.; Scheidt, W. R. *J. Am. Chem. Soc.* **1975**, *97*, 3247. (b) Kirner, J. F.; Reed, C. A.; Scheidt, W. R. *J. Am. Chem. Soc.* **1977**, *99*, 2557.

(26) At $[CH_3OH]$ above 3 M, the molar conductance increases rapidly and approaches the value observed for a 1:1 electrolyte, indicating that dissociation of $Mn(TPP)(CH_3OH)_2^+Cl^-$ occurs only at these higher concentrations of methanol.

(27) (a) Benesi, H. A.; Hildebrand, J. H. *J. Am. Chem. Soc.* **1949**, *71*, 2703. (b) Rossotti, F. J. C.; Rossotti, H. *The Determination of Stability Constants*; McGraw-Hill: New York, 1961; Chapter 13.

$$Mn^{III}(TPP)Cl + CH_3OH \rightleftharpoons Mn^{III}(TPP)(CH_3OH)Cl \quad K_1^{III} \quad (6)$$

$$Mn^{III}(TPP)Cl + 2CH_3OH \rightleftharpoons Mn^{III}(TPP)(CH_3OH)_2^+ Cl^- \quad \beta_2^{III} \quad (7)$$

M using two wavelengths each in the Soret band and low-energy visible regions are summarized in Table I. The result for eq 7 ($n = 2.2 \pm 0.2, \beta_2^{III} = 1.0 \pm 0.3\ M^{-2}$) shows no significant variation over 2 orders of magnitude of porphyrin concentration, which confirms the assumption that $Mn(TPP)(CH_3OH)_2^+Cl^-$ remains almost completely ion-paired at $[CH_3OH] < 3$ M. Although results for the 1:1 complex ($n = 0.8 \pm 0.3, K_1^{III} = 0.3 \pm 0.1\ M^{-1}$) are statistically no less significant than those for the 2:1 adduct, conclusions regarding this species are less secure because the small absorbance changes that accompany addition of the first molecule of CH_3OH make it difficult to obtain a reliable value of A_∞ for use in eq 5.[28] However, there is clear evidence for stepwise formation of 1:1 and 2:1 complexes because two independent sets of isosbestic points are observed during the titration: one at 466 and 487 nm that accompanies the decrease in the 476-nm Soret band when $[CH_3OH] = 0.0$–0.16 M (Figure 3A) and the second at 472 and 498 nm that accompanies the more dramatic spectral change at $[CH_3OH] \geq 0.4$ M (Figure 3B). We used the 466-nm isosbestic point and an alternate data analysis procedure[29] to obtain a value of $K_2^{III} = 3.4\ M^{-1}$ for coordination of a second molecule of CH_3OH to Mn(TPP)Cl

$$Mn^{III}(TPP)(CH_3OH)Cl + CH_3OH \rightleftharpoons Mn^{III}(TPP)(CH_3OH)_2^+ Cl^- \quad K_2^{III} \quad (8)$$

from which a result of $K_1^{III} = \beta_2^{III}/K_2^{III} = 0.3\ M^{-1}$ is calculated, in good agreement with Table I.

The equilibrium constants for reactions 6 and 7 and also that for bonding of CH_3OH to the Mn(II) electrode product (K_1^{II})

$$Mn^{II}(TPP)Cl^- + CH_3OH \rightleftharpoons Mn^{II}(TPP)(CH_3OH) + Cl^- \quad K_1^{II} \quad (9)$$

can be determined from the electrochemical data in Figure 2. If reactions 6, 7, and 9 control the distribution of Mn species in the III and II oxidation states, the half-wave potential for $Mn^{III/II}$ reduction as a function of CH_3OH concentration can be expressed as

$$E_{1/2} = (E_{1/2})_0 + 0.059 \log \left(\frac{1 + K_1^{II}[CH_3OH]/[Cl^-]}{1 + K_1^{III}[CH_3OH] + \beta_2^{III}[CH_3OH]^2} \right) \quad (10)$$

where $(E_{1/2})_0$ is the half-wave potential in absence of added CH_3OH (eq 1). At intermediate CH_3OH concentrations, eq 10 reduces to

$$E_{1/2} = (E_{1/2})_0 + 0.059 \log \left(\frac{1 + K_1^{II}[CH_3OH]/[Cl^-]}{1 + K_1^{III}[CH_3OH]} \right)$$

Provided $K_1^{II}/[Cl^-] > K_1^{III}$, this relation explains the initial positive shift in half-wave potential upon addition of CH_3OH. From values of $E_{1/2}$ recorded at $[CH_3OH] = 0.1$–0.5 M and $[Cl^-] = 0.1$ M in Figure 2 and the assumption that $K_1^{III} = 0.3\ M^{-1}$, a result of $K_1^{II} = 0.27 \pm 0.04\ M^{-1}$ is obtained. At large CH_3OH concentrations, eq 10 reduces to $E_{1/2} = (E_{1/2})_0 + 0.059 \log (K_1^{II}/\beta_2^{III}[CH_3OH][Cl^-])$, which is consistent with the subsequent shift of $E_{1/2}$ to negative values. The intersection of the negatively sloping data points in Figure 2 with $(E_{1/2})_0$ yields $K_1^{II}/\beta_2^{III}[Cl^-] = 2.4\ M^{-1}$, from which $\beta_2^{III} = 1.1\ M^{-2}$. Thus, the electrochemical results confirm the value of β_2^{III} determined spectrophotometrically. In Figure 2, the $Mn^{III/II}$ half-wave potential calculated from eq 10 with $(E_{1/2})_0 = -0.235$ V, $K_1^{II} = 0.4$, $K_1^{III} = 0.3\ M^{-1}$, $\beta_2^{III} = 1.0\ M^{-2}$, and $[Cl^-] = 0.1$ M is compared with the experimental result. The slightly larger value of K_1^{II} provides a better fit of the experimental data over the entire range of CH_3OH concentrations. The agreement between the measured and calculated responses confirms the model of CH_3OH coordination to the Mn^{II} and Mn^{III} states of Mn(TPP)Cl.[30]

Electrochemical determination of the equilibrium constants for reactions 6, 7, and 9 also was carried out at 241 K. Behavior similar to that illustrated in Figure 2 is observed; $E_{1/2}$ shifts first in the positive and then in the negative direction with increasing methanol concentration but with smaller slopes appropriate to the lower temperature. A significant difference is that CH_3OH appears to bond more strongly to both Mn^{II} and Mn^{III} at 241 K. The methanol concentrations at which the half-wave potential exhibits its initial positive displacement and its maximum value occur at lower values of $[CH_3OH]$ by ca. 1.0 log unit at this temperature. Values of $K_1^{II} = 3$, $K_1^{III} = 5\ M^{-1}$, and $\beta_2^{III} = 15\ M^{-2}$ were determined at 241 K.

Effect of CH_3OH Bonding on Electrooxidation of Mn(TPP)Cl. Figure 4 contains a conventional cyclic voltammogram recorded at a 1.6 mm diameter Pt electrode and a steady-state voltammogram recorded at a 25 μm diameter Pt microelectrode for electrooxidation of $Mn^{III}(TPP)Cl$ at 241 K in the absence of added methanol. Use of this lower temperature extends the positive potential limit of the solvent and enables two oxidation waves to be observed. The first occurs at $E_{1/2} = 1.22$ V and is chemically and electrochemically reversible ($i_{pc}/i_{pa} = 1$; $\Delta E_p = 50$ mV and is independent of scan rate). The second occurs at

Table I. Spectroscopic Determination of Formation Constants of CH_3OH Complexes of Mn(TPP)Cl[a]

conc,[b] M × 10^6	wavelength, nm	1:1[c] n	1:1[c] K_1^{III}, M^{-1}	2:1[d] n	2:1[d] β_2^{III}, M^{-2}
7.6	468			2.1	1.4
	476	0.6	0.5	1.7	1.1
14.2	468			2.5	1.1
	476	0.5	0.2	2.1	1.2
68	566	1.1	0.3	2.2	0.9
	600	0.8	0.2	2.3	0.8
850	566	1.1	0.3	2.2	0.5
	600	1.0	0.4	2.2	0.6
av (std dev)		0.8 (3)	0.3 (1)	2.2 (2)	1.0 (3)

[a] In $ClCH_2CH_2Cl$ with no added electrolyte. [b] Mn(TPP)Cl concentration. [c] From eq 5 at $[CH_3OH] = 0.05$–0.5 M. [d] From eq 5 at $[CH_3OH] = 0.5$–2 M.

(28) For our calculations, we assumed $Mn(TPP)(CH_3OH)Cl$ to have the same value of A_∞ as $Mn(TPP)(CH_3OH)_2^+$ at the indicated wavelength.

(29) The procedure involves analyzing data at the wavelength of the first isosbestic point (466 nm) under conditions where the second equilibrium predominates ($[CH_3OH] = 1$–3 M). This allows spectral changes associated with the second equilibrium to be isolated and an accurate value of K_2^{III} to be determined. The data are analyzed by plotting the function $(A - A_0)/(A_\infty - A)$ versus $[CH_3OH]$ under the above conditions, where A_0 is the initial absorbance, A_∞ is the absorbance of the fully formed 2:1 complex, and A is the absorbance of the equilibrium mixture. The slope of the plot is K_2^{III}. (a) Mu, X. H.; Schultz, F. A. In preparation. (b) Reference 27b, pp 278–9. (c) Drago, R. S.; Tanner, S. P.; Richman, R. M.; Long, J. R. *J. Am. Chem. Soc.* **1979**, *101*, 2897. (d) Drago, R. S.; Long, J. R.; Cosmano, R. *Inorg. Chem.* **1981**, *20*, 2920.

(30) However, it is evident that the agreement between observed and calculated results is not perfect. In particular, experimental points rise less rapidly and fall more quickly at small and large CH_3OH concentrations, respectively, than predicted by eq 10. We have not identified the reasons for these differences but believe they could result from variation in equilibrium constants with solvent composition or from small contributions of additional (e.g., ion-pair) equilibria not considered in our model.

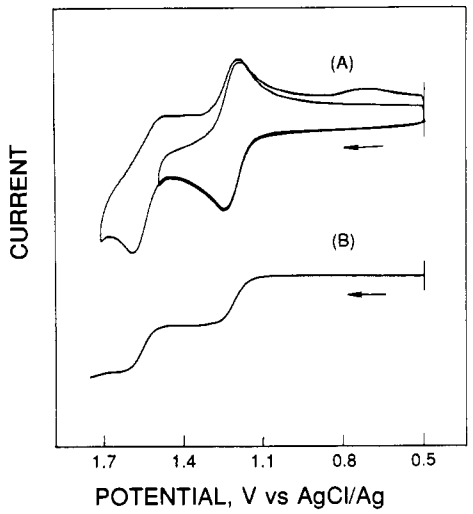

Figure 4. (A) Cyclic voltammogram at a 1.6 mm diameter Pt electrode (200 mV s^{-1}) and (B) steady-state voltammogram at a 25 μm diameter Pt microelectrode (20 mV s^{-1}) for oxidation of 8.5×10^{-4} M Mn^{III}(TPP)Cl at 241 K in CH_2ClCH_2Cl containing 0.1 M Bu_4NBF_4.

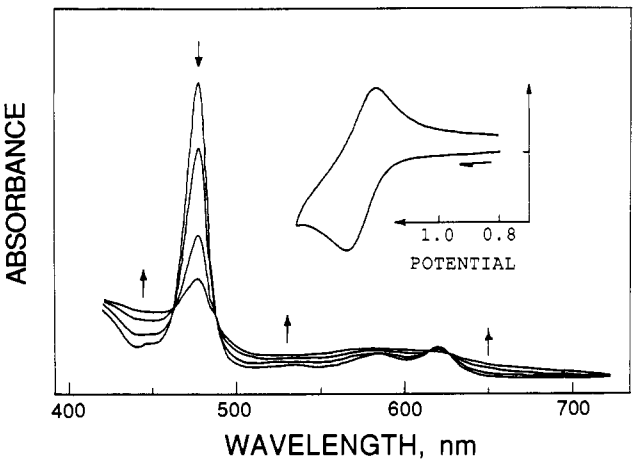

Figure 5. Visible spectra recorded during thin-layer cyclic voltammetric oxidation of 2.3×10^{-4} M Mn(TPP)Cl in $ClCH_2CH_2Cl$ containing 0.1 M Bu_4NBF_4. Inset: Thin-layer cyclic voltammogram recorded at a sweep rate of 5 mV s^{-1}.

$E_{1/2}$ = 1.56 V and is chemically and electrochemically quasi-reversible, as judged by a cathodic-to-anodic peak current ratio of less than unity, a scan rate dependent peak potential separation that is greater than the Nernst value of 48 mV, and a more gradual decline in the current of the microelectrode voltammogram.

The first oxidation wave was investigated by thin-layer spectroelectrochemistry at room temperature. Figure 5 shows that the Soret band decreases significantly in intensity and is replaced by a much less structured absorption as Mn(TPP)Cl is oxidized by one electron. On the basis of this behavior, the first oxidation wave is assigned to formation of a porphyrin π-cation radical:

$$Mn^{III}(TPP)Cl \rightleftharpoons Mn^{III}(TPP^{\bullet})Cl^{+} + e^{-} \quad (11)$$

Arasasingham and Bruice[24] reached a similar conclusion regarding the one-electron oxidation of Mn(TMP)Cl (TMP = tetramesitylporphyrin) in CH_2Cl_2. The product of the second oxidation of Mn(TPP)Cl could not be characterized spectroelectrochemically. However, we assign this process to a manganese-centered oxidation (eq 12) on the basis of its apparently slow electron-

$$Mn^{III}(TPP^{\bullet})Cl^{+} \rightleftharpoons Mn^{IV}(TPP^{\bullet})Cl^{2+} + e^{-} \quad (12)$$

transfer kinetics. We have noted[31] that when slow heterogeneous charge-transfer reactions are observed for metalloporphyrin species, these generally are associated with metal- rather than ring-centered events.

Figure 6 shows the effect of methanol addition on the electrochemistry of Mn(TPP)Cl at 241 K. The traces in the left-hand side of the figure pertain to its oxidation and are discussed in this section. The use of low temperature helps to diminish the effect of chemical reactions coupled to electron transfer, as indicated by the fact that the cyclic voltammetric currents retain diffusion-limited behavior (i_p proportional to $v^{1/2}$) in the presence of methanol. Thus, the voltammetric traces reflect the equilibrium composition of the solutions. Addition of CH_3OH causes the current of the initial oxidation reaction (wave 1, eq 11) to diminish. Concurrently, wave 2 appears at a potential between those of reactions 11 and 12. At larger CH_3OH concentrations, wave 1 vanishes and wave 2 increases in size until it achieves a height twice that of the first wave. The new wave occurs at a [CH_3OH]-independent half-wave potential of 1.31 V and is not chemically reversible, as judged by its small cathodic current and the appearance of an additional cathodic peak at 0.7 V on the reverse scan. Reaction 12 could not be observed after addition of CH_3OH because of a change in the positive potential limit.

The appearance of wave 2 and its increase in size parallel closely the conversion of Mn(TPP)Cl to its methanol-coordinated forms. We believe this wave represents oxidation of these CH_3OH-coordinated materials in equilibrium with Mn(TPP)Cl. In support of this argument, the heights of the microelectrode plateau currents corresponding to the oxidations at 1.22 V ($i_{L,1}$) and 1.31 V ($i_{L,2}$) are plotted as a function of CH_3OH concentration in Figure 7. Also plotted in this figure is the microelectrode plateau current ($i_{L,red}$) for metal-centered reduction of Mn(TPP)Cl under the same conditions. The decrease in $i_{L,1}$ and the increase in $i_{L,2}$ commence at CH_3OH concentrations where conversion of Mn(TPP)Cl to species **3** and **4** begins and continues until all **1** is converted to **4**. The correspondence between these parameters and the ultimate value of $i_{L,2}$ suggests that the CH_3OH-coordinated forms of Mn(TPP)Cl are oxidized by two electrons in wave 2 at the expense of the one-electron oxidation of Mn(TPP)Cl in wave 1.

$$Mn^{III}(TPP)(CH_3OH)Cl - 2e^{-} \rightarrow Mn^{IV}(TPP^{\bullet})(CH_3OH)Cl^{2+} \quad (13)$$

$$Mn^{III}(TPP)(CH_3OH)_2^{+} - 2e^{-} \rightarrow Mn^{IV}(TPP^{\bullet})(CH_3OH)_2^{3+} \quad (14)$$

Effect of CH_3OH Bonding on Apparent Kinetics of $Mn^{III/II}$ Reduction. Another effect of methanol coordination on the electrochemical behavior of Mn(TPP)Cl is illustrated by the steady-state and cyclic voltammograms on the right-hand side of Figure 6. Electroreduction of Mn(TPP)Cl in the absence of CH_3OH is kinetically slow, as indicated by the large peak potential separation in the cyclic voltammetry experiment and the drawn-out current–potential curve in the microelectrode experiment. Similar responses are observed at room temperature. We have attributed[32] this behavior to the large additional out-of-plane displacement (0.37 Å)[11] that the Mn atom experiences upon reduction from Mn^{III}(TPP)Cl to Mn^{II}(TPP)Cl^{-} and have conjectured that this structural change constitutes a sufficient inner-shell activation barrier to slow the rate of electron transfer. As methanol is added to the Mn(TPP)Cl solution, in Figure 6 the cyclic voltammetric peak potential separation decreases and the slope of the i–E curve in the microelectrode experiment increases. Both responses approach Nernstian behavior at large methanol concentrations. Figure 8 plots the change in ΔE_p for Mn(TP-

(31) Mu, X. H.; Schultz, F. A. *Inorg. Chem.* **1990**, *29*, 2877.

(32) Feng, D.; Schultz, F. A. *Inorg. Chem.* **1988**, *27*, 2144.

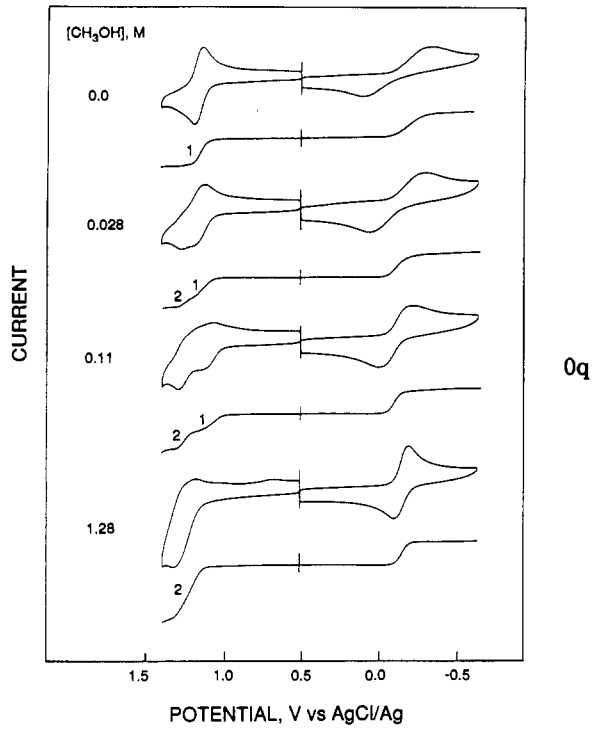

Figure 6. Cyclic voltammograms at a 1.6 mm diameter Pt electrode (200 mV s^{-1}) and steady-state voltammograms at a 25 μm diameter Pt microelectrode (20 mV s^{-1}) for oxidation and reduction of 8.5×10^{-4} M Mn(TPP)Cl at 241 K in $ClCH_2CH_2Cl$ containing 0.1 M Bu_4NBF_4 and 0.0, 0.028, 0.11, and 1.28 M CH_3OH.

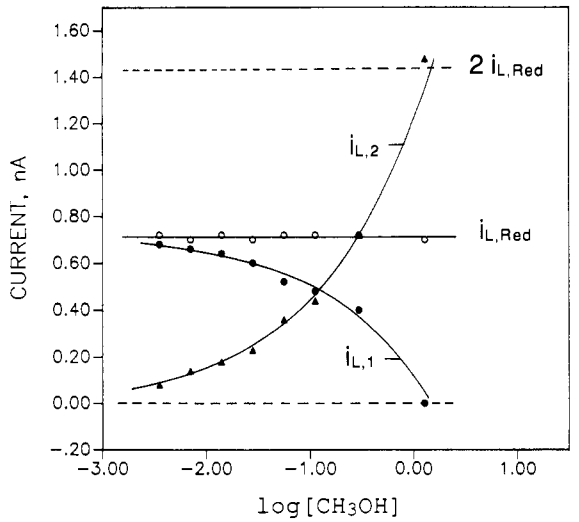

Figure 7. Steady-state currents observed at a 25 μm diameter Pt microelectrode as a function of CH_3OH concentration for reduction ($i_{L,red}$) and oxidation ($i_{L,1}$ and $i_{L,2}$) of 8.5×10^{-4} M Mn(TPP)Cl at 241 K and 20 mV s^{-1} in $ClCH_2CH_2Cl$ containing 0.1 M Bu_4NBF_4.

P)Cl reduction as a function of methanol concentration at room temperature. The majority of the change occurs at CH_3OH concentrations between 0.03 and 0.3 M.

Discussion

Effect of Methanol Bonding on Equilibrium Distributions, Cathodic Half-Reactions, and Apparent Kinetics of Metal-Centered Reduction of Mn(TPP)Cl. The influence of methanol bonding on the properties of Mn(TPP)Cl is clarified by definition of three regions within which different characteristic behaviors occur. These regions are bounded approximately by log [CH_3OH] = −1.0 and 0.0 at 296 K and −2.0 and −1.0 at 241 K. The predominant electrode half-reactions within each region are summarized in Table II. In region I, the electrochemistry of

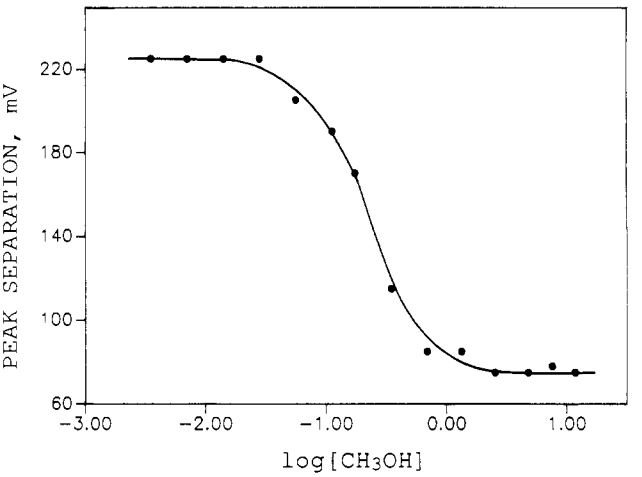

Figure 8. Cyclic voltammetric peak potential separation at 200 mV s^{-1} as a function of methanol concentration for metal-centered reduction of Mn(TPP)Cl at 296 K in $ClCH_2CH_2Cl$ containing 0.1 M Bu_4NBF_4.

Scheme I

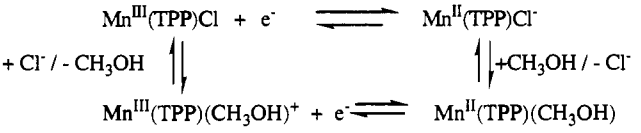

Mn(TPP)Cl is uninfluenced by methanol concentration. Its reduction proceeds by a kinetically slow metal-centered electron transfer. In region II, some axial ligation by CH_3OH occurs in the Mn^{III} state, and the electrode reactants are a mixture of species **1** and **3**. In region III, the bisligated complex **4** is the predominant Mn^{III} species. Mn(TPP)(CH_3OH) is the sole product of electrochemical reduction in the last two regions.

A significant feature in the cathodic electrochemistry of Mn(TPP)Cl is the observation that its metal-centered reduction potential shifts first in the positive and then in the negative direction with increasing CH_3OH concentration (Figure 2). This results from the greater affinity of the Mn^{II} state for a first molecule of CH_3OH and its preference to remain five-coordinate under conditions where Mn^{III} increases its coordination number to 6 by bonding two CH_3OH molecules. Consequently, at moderate methanol concentrations, the axial Cl^- ligand is replaced by CH_3OH upon reduction and the oxidizing strength of the metal center increases. At higher methanol concentrations, a CH_3OH ligand is lost upon reduction and the oxidizing strength of the metal decreases. This biphasic behavior illustrates how axial ligation can modulate metalloporphyrin redox potentials, a feature that may be useful in sustaining catalytic cycles based on the redox chemistry of these species.

Changes in axial ligation also influence the apparent kinetics of metal-centered reduction. One explanation of this behavior is that the inner-shell barrier to electron transfer is reduced by structural changes that occur when CH_3OH coordinates to Mn(TPP)Cl. Reduction of **1** to **5** is slow because it is accompanied by a large change (0.37 Å) in the metal atom out-of-plane distance. It is not clear what the magnitudes of the Franck–Condon barriers associated with the reductions of **3** and **4** to **6** should be. An argument could be made that they are smaller, because a smaller out-of-plane displacement might be anticipated in compound **6** versus compound **5** when CH_3OH replaces Cl^- as the axial ligand. However, the Mn atom is closer to the porphyrin plane in **3** and **4** than it is in **1**, which would make the barriers larger. It is important to notice that most of the increase in kinetics occurs before appreciable equilibrium concentrations of **3** and **4** are formed (Figure 8). Thus, it is likely that reduction of **1** proceeds

Table II. Electrode Reactions of Mn(TPP)Cl at Various Methanol Concentrations[a]

reduction	oxidation
region I $Mn^{III}(TPP)Cl + e^- \rightleftharpoons Mn^{II}(TPP)Cl^-$	region I $Mn^{III}(TPP)Cl - e^- \rightleftharpoons Mn^{III}(TPP^{\bullet})Cl^+$ $Mn^{III}(TPP^{\bullet})Cl^+ - e^- \rightleftharpoons Mn^{IV}(TPP^{\bullet})Cl^{2+}$
region II $Mn^{III}(TPP)Cl + CH_3OH + e^- \rightleftharpoons Mn^{II}(TPP)(CH_3OH) + Cl^-$ $Mn^{III}(TPP)(CH_3OH)Cl + e^- \rightleftharpoons Mn^{II}(TPP)(CH_3OH) + Cl^-$	region II $Mn^{III}(TPP)Cl - e^- \rightleftharpoons Mn^{III}(TPP^{\bullet})Cl^+$ $Mn^{III}(TPP)(CH_3OH)Cl - 2e^- \rightarrow Mn^{IV}(TPP^{\bullet})(CH_3OH)Cl^{2+}$ [b]
region III $Mn^{III}(TPP)(CH_3OH)_2^+ + e^- \rightleftharpoons Mn^{II}(TPP)(CH_3OH) + CH_3OH$	region III $Mn^{III}(TPP)(CH_3OH)_2^+ - 2e^- \rightarrow Mn^{IV}(TPP^{\bullet})(CH_3OH)_2^{3+}$ [b]

[a] Regions I–III correspond respectively to CH_3OH concentrations of <0.1, 0.1–1.0, and >1.0 M at 296 K and <0.01, 0.01–0.1, and >0.1 M at 241 K. [b] Initial electrode reaction product; chemical reaction occurs subsequent to charge transfer under these conditions.

by the electrochemical mechanism[33] shown in Scheme I. Facile kinetics of CH_3OH association and dissociation within Scheme I would serve to increase the apparent rate of electron transfer at the Mn center compared with the circumstance where no change in coordination environment occurs. Similar schemes would maintain rapid apparent kinetics once substantial equilibrium concentrations of **3** and **4** are formed.

Effect of Methanol Bonding on Anodic Half-Reactions. In region I, Mn(TPP)Cl oxidation proceeds by sequential ligand- and metal-centered charge transfers that are independent of $[CH_3OH]$. However, significant changes occur in the oxidative electrochemistry of Mn(TPP)Cl at larger CH_3OH concentrations. These changes affect oxidations at both the metal and the ring. In regions II and III, the porphyrin-centered oxidation wave (eq 11) diminishes and is replaced by an irreversible two-electron oxidation (eq 13 or 14) at a more positive potential. The two-electron transfer likely consists of overlapping one-electron transfers, which implies that the potential of porphyrin-centered oxidation has been shifted in the positive direction and that of metal-centered oxidation in the negative direction by CH_3OH coordination. The latter observation is anticipated from the greater donor strength provided by two CH_3OH molecules versus one chloride ion and has been observed following coordination of oxygen donor ligands to manganese(III) porphyrins.[24] Reasons for the positive shift in the porphyrin-centered oxidation potential are less obvious. One interpretation is that hydrogen-bond interactions between the hydroxyl protons of coordinated CH_3OH and TPP stabilize the porphyrin redox orbital and shift its potential to a more positive value. A second explanation is related to the observation that methanol coordination forces the Mn atom back into the porphyrin plane (structures **3** and **4**) and results in less distortion of the porphyrin core. Fajer et al.[34] have shown that the HOMO of sterically distorted porphyrins is destabilized relative to that of planar systems, making the compounds easier to oxidize. Methanol coordination would have the effect of flattening the porphyrin ring and increasing its oxidation potential.

Finally, we note that the current associated with wave 1 in Figure 6 corresponds closely to the equilibrium concentration of uncomplexed Mn(TPP)Cl. This fact indicates that dissociation of CH_3OH from **3** or **4** is too slow to contribute significantly to the oxidation current via a CE mechanism[35] such as

$$Mn^{III}(TPP)(CH_3OH)Cl \rightleftharpoons Mn^{III}(TPP)Cl + CH_3OH \quad (15)$$

$$Mn^{III}(TPP)Cl - e^- \rightleftharpoons Mn^{III}(TPP^{\bullet})Cl^+ \quad (16)$$

An upper limit of 1.0×10^{-2} s^{-1} is calculated for the forward rate constant of eq 15 at 241 K under the assumption that the diffusion-limited current of Mn(TPP)Cl oxidation is enhanced ≤20% by the chemical step. Thus, dissociation of CH_3OH from the Mn^{III} center appears slow when compared with analogous reactions of other metalloporphyrins.[36]

Acknowledgment. Support of this research by the National Science Foundation (Grant No. CHE-8718013) is gratefully acknowledged, as are helpful conversations with Dr. Philip Crawford.

(33) Evans, D. H. *Chem. Rev.* **1990**, *90*, 739.
(34) Barkigia, K. M.; Chantranupong, L.; Smith, K. M.; Fajer, J. *J. Am. Chem. Soc.* **1988**, *110*, 7566. (b) Barkigia, K. M.; Berber, D. M.; Fajer, J.; Medforth, C. J.; Renner, M. W.; Smith, K. M. *J. Am. Chem. Soc.* **1990**, *112*, 8851.
(35) Nicholson, R. S.; Shain, I. *Anal. Chem.* **1964**, *36*, 706.
(36) (a) Doeff, M. M.; Sweigart, D. A. *Inorg. Chem.* **1982**, *21*, 3699. (b) Nakamura, M. *Inorg. Chim. Acta* **1989**, *161*, 73.